Synthesis And Properties Of Clay-Zro_2-Cellulose Fibre-Reinforced Polymeric Nano-Hybrids

M. McGrath[1], W. Vilaiphand[1], S. Vaihola[1], A. Lopez[1], I.M. Low[1] and B.A. Latella[2]
[1]Materials Research Group, Department of Applied Physics, Curtin University of Technology, GPO Box U1987, Perth, WA 6845
[2]Materials Division, ANSTO, PMB-1, Menai, NSW 2234

ABSTRACT: Epoxy nano-hybrids reinforced with cellulose fibre (CF), nano-kaolinite (K), and micro-ZrO_2 (Z) have been synthesized. The influence of CF/K/Z dispersions on the mechanical properties of these hybrids have been characterized in terms of elastic modulus, hardness, flexural strength, fracture toughness and indentation responses. This new but cost-effective approach has been developed to improve the physical and mechanical properties of polymeric materials without adversely affecting their processing characteristics. The mechanism of reinforcement in these organic/inorganic nanohybrid materials has been investigated. The micromechanisms of toughening and failure processes are identified and discussed in the light of observed nano- and micro-structures.

1 INTRODUCTION

Recent advances in polymer–clay nanocomposites due to the pioneering work of researchers at Toyota on nylon-6/clay nanocomposites have demonstrated an improvement in both physical and mechanical properties [Kojima *et al.* 1993; Usuki *et al.* 1993]. Because of the nanoscale structure, polymer–clay nanocomposites possess unique properties which include an improvement in mechanical (modulus, strength, toughness), thermal (thermal stability, decomposition, flammability, coefficient of thermal expansion), and physical (permeability, optical, dielectric, shrinkage) properties [Park & Jana, 2003; Isik *et al.*, 2003; Ma *et al.*, 2003; Kornmann *et al.*, 2001; Fu & Qutubuddin, 2000]. Nanocomposites have been demonstrated with many polymers of different polarities including polystyrene, polycaprolactone, poly(ethylene oxide), poly(butylene terephthalate), polymethylmethacrylate, polyamide, polyimide, polyester, polyether, epoxy, polysiloxane, and polyurethane.

Similarly, cellulose and other natural fibres are increasingly being used as reinforcements for enhancing the strength and fracture resistance of polymeric matrices because of their low density, low cost, renewability and recyclability as well as excellent mechanical characteristics that include flexibility, high specific strength and high specific modulus [Bledzki & Gassan, 1999; Marsh, 2003; Low *et al.*, 1995; Rowles *et al.* 1999; Lawrence *et al.*, 2000]. These unique properties are particularly desirable in applications as composite materials for automobiles, armour, sports, and marine industries.

The emergence of a new approach in the design of layered ceramic-based composites has now provided a strategy for designing materials with high strength and high toughness. These structures have an outermost homogeneous layer to provide strength or wear resistance, and an underlying heterogeneous layer to provide toughness [An *et al.*, 1996; Padture 1995]. Unlike more traditional layered structures which promote toughness by interlayer crack deflection or strength by incorporating macroscopic compressive residual stresses, the new approach deliberately seeks to produce strong interlayer bonding and to eliminate residual macroscopic stresses. Accordingly, any attendant counterproductive effects of weak interlayers and residual stresses from delamination failures can be avoided.

In this paper, we propose a modification on this alternative approach to design nano-hybrids in which microstructural elements are tailored to provide both nano- and fibre-dispersed compositions and generate different modes of strengthening and toughening. The basic idea is to produce an outer epoxy layer dispersed with kaolin and ZrO_2 for strength and wear resistance, and with underlayers of cellulose-fibre reinforced epoxy for toughness and damage tolerance. An attractive advantage of the proposed nanohybrids is the fact that such enhancements can be achieved at much lower volume fractions when compared with their conventional fiber-reinforced composites. Such low volume fractions offer the potential for the incorporation of nanoscale elements into existing polymer resins without requiring significant modification of existing processing techniques, providing for low-cost property improvements for commodity polymers and increased tailorability options for advanced composite matrices. This new but cost-effective approach has been developed to improve the physical and mechanical properties of polymeric materials without adversely affecting their processing characteristics. The mechanism of reinforcement in these nano-hybrids has been studied in terms of hardness, strength, elastic modulus, fracture toughness, and indentation responses. The micromechanisms of strengthening, toughening and failure processes are identified and discussed in the light of observed nano- and micro-structures.

2 EXPERIMENTAL PROCEDURE

Nano-sized (~100 nm) kaolinite (K), micro-sized (~10-50 μm) ZrO_2 (Z) and cellulose-fibre performs (CF) were used to fabricate K/Z/CF-reinforced epoxy nanocomposites. Softwood aspen (*Pinus radiata*) mats in the form of bleached chemithermomechanical pulp (CTMP) were used as reinforcing fibre preforms. The aspect ratio of the CF was approximately 5-15.

Samples were prepared by initially casting a thin (~1.0 mm) bottom-layer of epoxy/K/Z mixture in a greased silicone rubber mould. Three sheets of epoxy- soaked CTMP fibre-mat were then laid down, followed by a top-layer of epoxy/K/Z. For comparison purposes, samples without either K or Z dispersion were also prepared to evaluate its effect on the mechanical performance. All the samples were cured overnight at room temperature. Rectangular bars and compact-tension samples were cut for the measurements of elastic modulus, hardness, flexural strength, fracture toughness, and crack-growth resistance (R-curve). Table 1 shows the composition of the various samples and their typical microstructures are shown in Figure 1.

Table 1: The composition of the various samples made.

Sample	Composition
ECF	Epoxy (40%), Cellulose Fibre (60%)
EKCF	Epoxy (30%), Kaolinite (20 wt%), Cellulose Fibre (50%)
EKZCF	Epoxy (30%), Kaolinite + ZrO_2 (20 wt%), Cellulose Fibre (50%)
EZCF	Epoxy (30%0, ZrO_2 (20 wt%), Cellulose Fibre (50%)

(a) (b)

Fig. 1: Cross-section view of the microstructure for (a) EKCF and (b) EKZCF. Arrows indicate air-bubbles trapped within the matrix. Large agglomerates of kaolinite can be seen at the top end of the EK layer. (Mag. 100×)

The flexural strength (σ_F), flexural modulus (E_F), strain at break (ε_B) and fracture toughness (K_{1c}) were measured using the three-point bend samples (50 mm × 10 mm × 8 mm) with a span of 20 or 40 mm [Low & Mai, 1992]. A Grindo-Sonic tester was also used to measure the elastic modulus (E_S) of rectangular bar samples with similar dimensions. The crack-growth resistance or R-curve of the samples was evaluated using compact-tension specimens (50 mm × 48 mm × 8 mm) with a clip-gauge to monitor the crack-opening displacement. Samples for indentation tests and optical microscopy were resin-mounted and polished with diamond paste down to 1 μm with a Struers Pedemat auto-polisher. The Vickers hardness measurements were performed with a Zwick microhardness tester. The lengths of the diagonal ($2a$) were used to calculate the hardness, determined as $H_v = P/2a^2$, where *P (10-100N)* is the load used. A Nikon microscope with a CCD camera was used to observe the microstructures of the various samples.

3 RESULTS AND DISCUSSION

The mechanical properties of the various samples are summarized in Table 2. Several interesting features are worth noting. Firstly, the presence of either kaolinite or ZrO_2 or both does not appear to improve the flexural strength or the flexural modulus of the samples but reduce it instead due to air-bubbles being trapped within the microstructure. Secondly, the strain at break, hardness, and fracture toughness are all observed to have increased as a result of the addition of either kaolinite or ZrO_2 or both. Thirdly, no radial cracks were observed during the indentation tests, even at the maximum load used. Lastly, the values of elastic modulus (E_S) as measured by the Grindo-Sonic tester are much higher than the values of E_F as measured by three-point bending.

Table 2: Mechanical properties of the various samples.

Sample	σ_F (MPa)	ε_B (%)	H_V (GPa)	E_F (GPa)	E_S (GPa)	K_{IC} (MPa.√m)
ECF	94.7 ± 6.2	8.8 ± 0.9	0.16 ± 0.01	1.6 ± 0.1	4.8 ± 0.2	3.1 ± 0.1
EKCF	64.2 ± 8.2	9.3 ± 1.6	0.17 ± 0.01	0.8 ± 0.1	5.3 ± 0.2	3.7 ± 0.1
EKZCF	79.0 ± 8.7	12.5 ± 0.8	0.18 ± 0.01	0.9 ± 0.1	5.7 ± 0.2	3.4 ± 0.1
EZCF	88.7 ± 7.9	10.2 ± 0.1	0.19 ± 0.02	1.2 ± 0.2	5.9 ± 0.2	3.2 ± 0.1

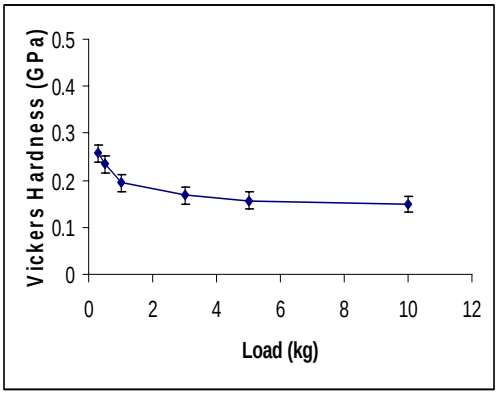

Fig. 2: Variation of hardness versus load for sample EZCF

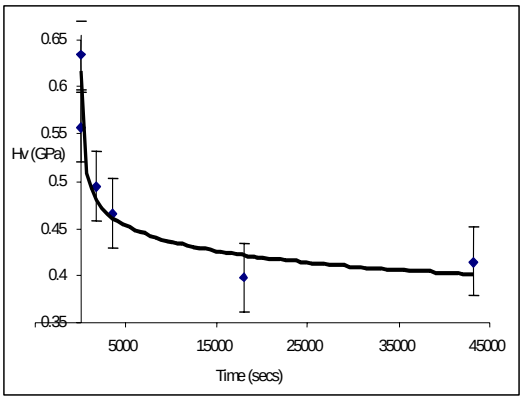

Fig. 3: Variation of hardness versus time for sample EKCF

Figure 2 shows the variation of hardness as a function of load for the ZrO_2-epoxy layer in sample EZCF. There is clearly a significant display of load-dependent hardness. This phenomenon is also apparent for the kaolinite-epoxy (sample EKCF) and the kaolinite-ZrO_2-epoxy layer (sample EKZCF) although not as pronounced. In contrast, this phenomenon was not observed for the CF-

epoxy layer of all samples. This load-independent hardness characteristic can be attributed to an indentation size effect [Low, 1998] or the agglomeration of particles. At small loads, the contact dimension ($2a$) of Vickers impression is comparable with the size of large agglomerate and the hardness measures its properties; when $2a$ becomes much larger than the agglomerate size at high loads, the hardness measures the "bulk" properties, with more agglomerate/epoxy interfaces oriented for deformation by plastic-shear and viscoelastic flow. It follows that this phenomenon will disappear if the fine particles can be uniformly dispersed within the epoxy matrix without forming large agglomerates.

It is interesting to note that no indentation radial cracks were observed on the surface of the individual layers, even at the maximum load used. The absence of these cracks can be ascribed to both low hardness (H_v) and high critical load (P_c) to initiate cracks (Lawn, 1993), where P_c is proportional to (K_{IC}^4/H_v^3). However, extensive damage due to interfacial-shear debonding and damage was seen in the CF/epoxy layer but not in kaolin/epoxy layer. The reasons for the apparent absence of any interfacial damage in the kaolin-epoxy, ZrO_2-epoxy or kaolin-ZrO_2-epoxy layer remain unclear. It is postulated that the thermal expansion mismatch in these layers may be favourable to minimize the formation of any undesirable residual stresses which might cause interfacial debonding.

The viscoelastic deformation of the kaolinite-epoxy layer in sample EKCF during indentation is clearly revealed in Fig. 3 which shows the variation of hardness as a function of loading time. Over a period of 1 h, the rate of reduction in hardness due to creep was very rapid but became more gradual after that. This suggests that during loading, the size of the indent increased with time as a result of viscoelastic flow and relaxation processes. It is postulated that in addition to the intrinsic viscoelastic flow and relaxation processes (Low, 1998), an expanding zone of microdamage within the CF-reinforced epoxy layer due to interfacial debonding is contributing to the observed creep process (Fig. 4). The presence of CF has acted as sites of stress-concentration and shear-deformation. In effect, the presence of these fillers in large amount has modified the intrinsic viscoelastic property of epoxy resin, rendering it more susceptible to shear-induced deformation at the CF-matrix interfaces. This mode of shear-deformation may impart an improvement in fracture resistance to the otherwise brittle epoxy resin.

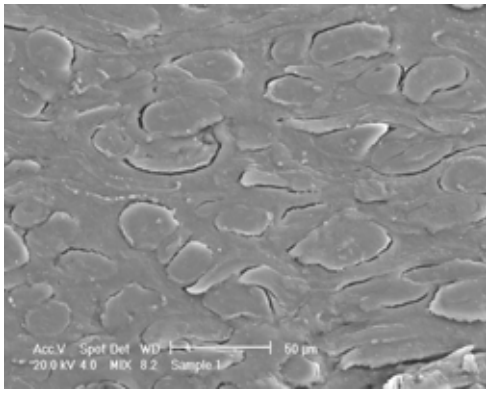

Fig. 4: SEM of the CE-epoxy layer showing extensive interfacial debonding.

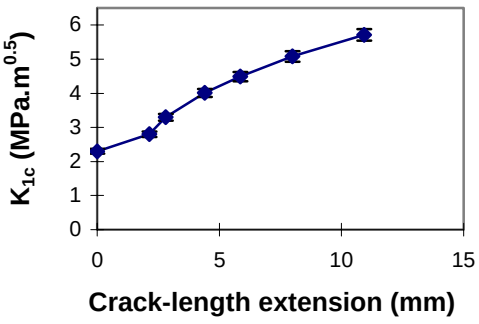

Fig. 5: Display of crack-growth resistance or R-curve in sample EKCF.

The fracture properties of all samples show characteristics of quasi-plasticity in the CF-epoxy layer; namely large scale shear deformation and the absence of macrocrack systems but the presence of extensive microdamage due to interfacial debonding. The deformation is accommodated by the buckling of CF and plastic shear at the CF-epoxy interfaces which prevent the nucleation of

subcritical voids or microcracks. The primary stage of damage involves extensive sliding between CF/epoxy interfaces resulting in surface uplift, debonding, and interfacial microcracking. Microcracks are facilitated by the presence of a large thermal expansion mismatch and initiated as a result of this sliding process which generates intense stresses. The display of crack-growth resistance or R-curve in sample EKCF is shown in Fig. 5. A similar phenomenon is also observed for samples ECF, EKZCF and EZCF. The origin of this phenomenon is attributed to an expanding crack-bridging zone at the wake of advancing crack-tip and extensive fibre pull-outs (Fig. 6) in sample ECF as well as crack-tip deflection (Fig. 7) in samples EKCF, EZCF and EKZCF, thus resulting in a tortuous and discontinuous crack-path.

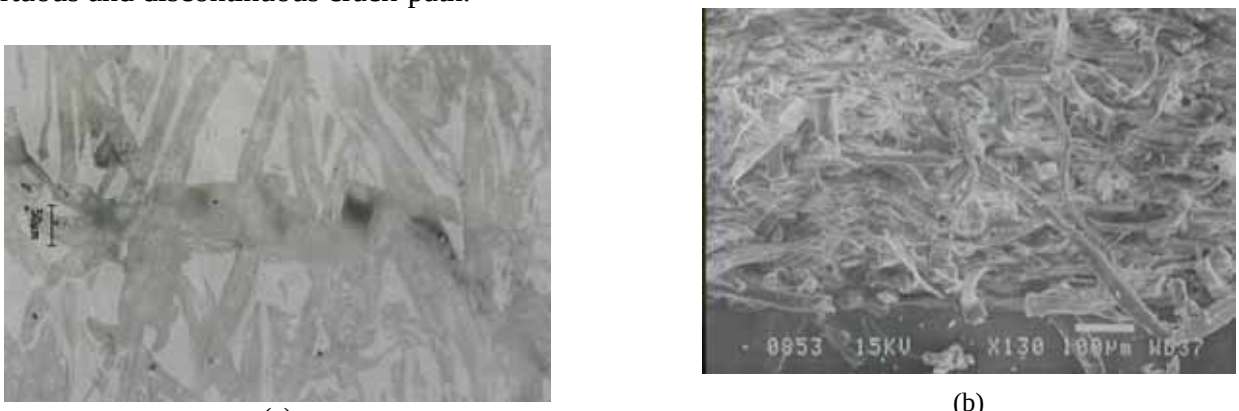

(a) (b)

Fig.6: Typical displays of (a) crack-bridging zone and (b) fibre pull-outs within the CF-epoxy layer.

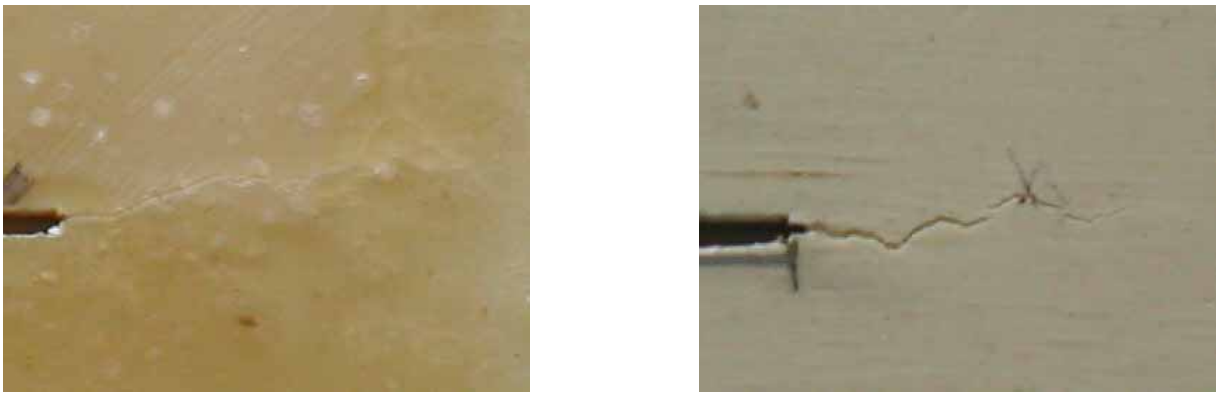

(a) (b)

Fig.7: Display of crack-tip deflection in sample (a) EKCF, and (b) EKZCF. (Mag. 2×)

Observations show stress-whitening at the crack tip, which on closer examination reveals extensive microdamage which is associated with debonding at the CF/epoxy interfaces, cavitation or microcraking, and the bridging, pullout, and fracture of the fibres. The formation of the damage zone ahead of an advancing crack-tip suggests that its propagation is achieved through the linking up of the expanding voids or microcracks with the advancing main crack. Avoidance of fibres and particulates by the advancing crack-tip is accomplished by the initial tilting and subsequent twisting of the crack front between the particulates or fibres, thus resulting in a non-planar crack-path. These complex energy dissipative processes are responsible for improving the fracture toughness and the display of crack-growth resistance (ie. R-curve) of all samples listed in Table 2. The toughening mechanisms described above are also reflected in other damage-tolerant materials such as short-fibre reinforced thermoplastics (Jang & Lieu, 1985) rubber-modified fibre epoxy hybrids (Low *et al.*, 1987, 1992), and cellulose-fibre reinforced cements (Mai & Hakeem, 1984; Mai *et al.*, 1984).

ACKNOWLEDGMENTS

IML is grateful to the ARC (LX0242352) and AINSE (AINGRA04181) for financial support, and to Dr. B. Lawn and Dr. Y. Zhang of NIST for technical help and access to their testing facility.

REFERENCES

An, L., Chan, H.M., Padture, N.P. & Lawn, B.R. Damage-resistant alumina-based layer composites, *J. Mater. Res*. **11,** 204 (1996)

Bledzki, A.K. & Gassan, J. Composites reinforced with cellulose-based fibres, *Prog. Polym. Sci*., **24**, 221 (1999)

Fu, X. & Qutubuddin, S. Synthesis of polystyrene–clay nanocomposites, *Mater. Lett.* **42**, 12 (2000)

Isik, I., Yilmazer, U. & Bayram, G. Impact modified epoxy/montmorillonite nanocomposites: Synthesis and characterization, *Polymer*, **44**, 6371 (2003)

Jang, B.Z. & Lieu, Y.K. *J. Appl. Polym. Sci*. **30**, 3925 (1985)

Kojima, Y., Usuki, A., Kawasumi, M., Okada,A., Fukushima, Y., Kurauchi, T. and Kamigaito, Mechanical properties of Nylon 6-clay hybrid, *J. Mater. Res.* **8**, 1185 (1993)

Kornmann, X., Lindberg, H. & Berglund, L.A. Synthesis of epoxy–clay nanocomposites: Influence of the nature of the clay on structure, *Polymer*, **42**, 1303 (2001)

Lawn, B.R. *Fracture of Brittle Solids*, Cambridge University Press, Cambridge, 1993.

Lawrence, D., Paglia, G. & Low, I.M. Indentation responses and damage of polymeric composites, *Proc. Structural Integrity and Fracture 2000*, (Ed. G. Heness), 29-30 June 2000, UTS, pp.119-127. (2000)

Low, I.M., Mai, Y.W., Bandyopadhayay & Silva, V.M. New toughened hybrid epoxies. *Materials Forum*. **10**, 241 (1987)

Low, I.M., Bandyopadhayay & Mai, Y.W. On hybrid toughened epoxy resins. *Polym. Int*. **27**, 131 (1992)

Low, I.M. & Mai, Y.W. Fracture properties and failure mechanisms in pure and toughened epoxy resins. Chapter 3 in Handbooks of Ceramics & Composite Materials, Vol.2: Mechanical properties & specialty applications, Edited by N.P. Cheremisinoff, Marcel Dekker Publishers, New York, pp105-160 (1992)

Low, I.M., Schmidt, P. Lane, J. & McGrath, M. Properties of rubber-modified cellulose-fibre/epoxy laminates, *J. Appl. Polym. Sci*. **54**, 2191 (1994)

Low, I.M., Schmidt, P. & Lane, J. Synthesis and properties of cellulose-fibre/epoxy laminates, *J. Mater. Sci. Lett*. **14**, 170 (1995)

Low, I.M. Effects of load and time on the hardness of a viscoelastic polymer, Mater. Res. Bull. 33, 1753 (1998)

Ma, J., Xu, J. Ren, J-H. Yu, Z-Z & Mai, Y-W. A new approach to polymer/montmorillonite nanocomposites, Polymer, **44**, 4619 (2003)

Mai, Y.W & Hakeem, M.I. *J. Mater. Sci. Lett*. **3**, 127 (1984)

Mai, Y.W., Hakeem, M.I. & Cottrell, B. *J. Mater. Sci*. **19**, 501 (1984)

Marsh, G. Next step for automotive materials, *MaterialsToday* **6**, 36 (2003)

Padture, N.P., Pender, D.C., Wuttiphan, S. & Lawn, B.R. In-situ processing of silicon carbide layer structures. *J. Am. Ceram. Soc*. **78**, 3160 (1995)

Park, J.H. & Jana, S.C. The relationship between nano- and micro-structures and mechanical properties in PMMA–epoxy–nanoclay composites, *Polymer*, **44**, 2091 (2003)

Rowles, M., Lawrence, D., Low, I.M., Schmidt, P. & Lane, J. Indentation responses and micromechanisms of failure in cellulose fibre/mylar/epoxy laminates, *Proc. Int. Workshop on Fracture Mechanics & Advanced Engineering Materials*, (Eds. L. Ye & Y.W. Mai), 8-10 Dec. 1999, Sydney University, pp.343-50 (1999)

Usuki, A., Kojima, Y., Kawasumi, M., Okada,A., Fukushima, Y., Kurauchi, T.,

and Kamigaito, Synthesis of Nylon 6-clay hybrid, *J. Mater. Res.* **8**, 1179 (1993)